Melanopsin- and L-cone–induced pupil constriction is inhibited by S- and M-cones in humans

Tom Woelders[a,1], Thomas Leenheers[a], Marijke C. M. Gordijn[a,b], Roelof A. Hut[a], Domien G. M. Beersma[a], and Emma J. Wams[a]

[a]Chronobiology Unit, Groningen Institute for Evolutionary Life Sciences, 9700CC Groningen, The Netherlands; and [b]Chrono@Work, 9743AD Groningen, The Netherlands

Edited by Joseph S. Takahashi, Howard Hughes Medical Institute and University of Texas Southwestern Medical Center, Dallas, TX, and approved December 8, 2017 (received for review September 15, 2017)

The human retina contains five photoreceptor types: rods; short (S)-, mid (M)-, and long (L)-wavelength–sensitive cones; and melanopsin-expressing ganglion cells. Recently, it has been shown that selective increments in M-cone activation are paradoxically perceived as brightness decrements, as opposed to L-cone increments. Here we show that similar effects are also observed in the pupillary light response, whereby M-cone or S-cone increments lead to pupil dilation whereas L-cone or melanopic illuminance increments resulted in pupil constriction. Additionally, intermittent photoreceptor activation increased pupil constriction over a 30-min interval. Modulation of L-cone or melanopic illuminance within the 0.25–4-Hz frequency range resulted in more sustained pupillary constriction than light of constant intensity. Opposite results were found for S-cone and M-cone modulations (2 Hz), mirroring the dichotomy observed in the transient responses. The transient and sustained pupillary light responses therefore suggest that S- and M-cones provide inhibitory input to the pupillary control system when selectively activated, whereas L-cones and melanopsin response fulfill an excitatory role. These findings provide insight into functional networks in the human retina and the effect of color-coding in nonvisual responses to light, and imply that nonvisual and visual brightness discrimination may share a common pathway that starts in the retina.

human pupillary light response | silent substitution | cones | melanopsin | ipRGC

The primate retina contains rods and three types of cones defined by their short-, mid-, and long-wavelength spectral sensitivity (henceforth S-, M-, and L-cones, respectively). Light information travels from the photoreceptive layer down to the ganglion cell layer, which eventually relays light information to the brain (reviewed in ref. 1). The ganglion cells that are involved in visual perception project basic information on color and luminance provided by the photoreceptors that indirectly innervate them. There are three major classes of retinal ganglion cells (RGCs) involved in visual color and/or luminance coding: the parasol cells, the midget ganglion cells, and the bistratified ganglion cells. Parasol cells are involved in luminance coding, with responses mainly mediated by a summation of M- and L-cone activation (L+M). Midget ganglion cells are involved in red/green color discrimination by comparing activation originating from L-cones and M-cones (+L − M or +M − L). Finally, the bistratified ganglion cell is thought to be involved in encoding color on the blue/yellow scale in an S − (L+M) manner. These cells thus receive excitatory input from the S-cones while receiving inhibitory input from a mixture of M- and L-cones. Besides its image forming function, light also elicits nonvisual effects such as the pupillary light response. Light information is relayed to brain areas involved in nonvisual responses via a specialized subset of RGCs that are intrinsically photosensitive by expressing melanopsin (2, 3). In the primate retina, intrinsically photosensitive RGCs (ipRGCs) have been shown to encode color on a blue/yellow scale, much like the bistratified retinal ganglion cells, but ipRGCs have been shown to receive input in an (L+M) − S opponent manner (4). The human pupillary light response seems to reflect this retinal wiring, as S-cone illuminance increments result in paradoxical pupil dilations (5).

To study the contribution of one photoreceptor type, the silent substitution method (6) can be employed. This method allows for selective modulation of the photoreceptor channel of interest. Any change in downstream neural processes is then a direct consequence of modulating the pathways in which the selected photoreceptor is involved. This is achieved by designing two spectra that are indistinguishable for all but one photoreceptor type. Temporally alternating these two spectra will then result in a selective modulation of the photoreceptor for which the transition is nonsilent. For example, a selective increment of M-cone activation will change the ratio between L- and M-cone stimulation, which will then alter the output of the associated midget ganglion cells, shifting the perceived stimulus color along the red/green scale. This method has recently been used to show that selective decrements in M-cone illuminance are paradoxically perceived as brightness increments (7). M-cone square-wave modulations furthermore produce electroretinogram (ERG) traces that are in opposite phase with traces resulting from L-cone (or L+M-cone) modulations (8, 9), which has also been shown in visually evoked potentials (VEPs) recorded at occipital scalp locations (10). Thus, at different levels of visual processing, M-cone increments are perceived as brightness decrements,

Significance

Human retinas contain five light-responsive cell types: rods; short (S)-, mid (M)-, and long (L)-wavelength–sensitive cones; and melanopsin-expressing ganglion cells. Intrinsically light-sensitive retinal ganglion cells (RGCs) also relay rod and cone information to brain areas involved in nonvisual responses, such as pupil constriction. Cones allow for visual color discrimination. How cone-dependent color discrimination affects nonvisual responses is poorly understood. We show that selectively activating L-cones or melanopsin constricts the pupil whereas S- or M-cone activation paradoxically dilates the pupil. Intrinsically photosensitive RGCs therefore appear to signal color on yellow/blue and red/green scales, with blue and green cone shifts being processed as brightness decrements. These findings are crucial in understanding brightness coding for visual and nonvisual responses such as circadian entrainment and alerting effects of light.

Author contributions: T.W., M.C.M.G., R.A.H., D.G.M.B., and E.J.W. designed research; T.W. and T.L. performed research; T.W. analyzed data; and T.W. wrote the paper.

The authors declare no conflict of interest.

This article is a PNAS Direct Submission.

[1]To whom correspondence should be addressed. Email: t.woelders@rug.nl.

This article contains supporting information online at www.pnas.org/lookup/suppl/doi:10.1073/pnas.1716281115/-/DCSupplemental.

whereas L-cone increments and L+M increments are perceived as brightness increments.

Although red/green color-opponent ipRGCs have not been described in the primate retina to our knowledge, it is interesting to test whether M-cone decrements result in paradoxical pupil constrictions, congruent with the aforementioned psychophysical, ERG, and VEP results. We therefore measured pupillary light responses in a silent substitution protocol. Contrary to the previously mentioned studies, we accounted for not only the three cone types in the human retina (i.e., triple silent substitution), but also the spectral sensitivity of melanopsin. With a peak absorbance at 480 nm (3), the spectral sensitivity of melanopsin overlaps substantially with those of S- and M-cones, such that, under triple silent substitution, the effects resulting from isolated S- or M-cone modulations may be confounded by concomitant melanopsin modulations. This approach thus allows for a selective square-wave modulation of isolated S-, M-, L-cone or melanopsin responses while maintaining a constant response for the remaining three receptor channels. The first purpose of this study was therefore to test how the human pupil responds to transient changes in photoreceptor-specific illuminance to provide insight into the retinal pathways involved in nonvisual brightness coding mediated by ipRGCs.

Another interesting phenomenon regarding brightness coding is that flickering light may appear brighter than light of constant intensity, also known as the Brücke–Bartley effect (11). Similar effects have recently been described for the pupillary light response (12). During prolonged exposure to light of constant intensity (~30 min), the pupil gradually dilates toward the dark-adapted diameter (pupillary escape) after an initial constriction at lights on, suggesting that encoded brightness gradually decays as a result of light-adaptation in cones. This pupillary escape is countered by presenting the light in a flickering (0.1–8 Hz) manner (12, 13), suggesting that a high level of encoded brightness is sustained in response to flickering light. These effects may be explained by considering retinal adaptation: by repeatedly allowing the cone-signaling pathway to dark-adapt, the response to each subsequent light pulse is increased, resulting in an increased overall contribution of these pathways to the sustained pupillary light response (effectively countering the effects of light-adaptation that results in pupillary escape under constant illumination). By using whole-cell recordings of mouse ipRGCs, it has been shown that ipRGC spiking rate increases during exposure to flickering on/off light in comparison with light of constant intensity (13), suggesting that increased nonvisual light responses to flickering light emerge at the retinal level. Although square-wave temporal modulation of one photoreceptor type may not cause complete dark-adaptation at each cycle, it will increase its response to each photoreceptor-specific illuminance increment. The silent substitution method thus allows for testing the effect of intermittent stimulation for each photoreceptor type separately, which may yield different results than those obtained under on/off flickering light exposure, in which all photoreceptors are modulated in concert. Given the inhibitory input of S-cones to ipRGCs in primates and the inhibitory nature of M-cones in subjective brightness perception in humans, it may be expected that enhanced S- and M-cone activation might paradoxically stimulate pupil dilation as measured by increased pupillary escape. The second question we address in this study is whether an increased time-averaged activity of photoreceptor channels (by effectively countering light-adaptation) decreases or increases encoded brightness over the time course of 30 min, for which pupillary escape is taken as a proxy. We expect that pupillary escape will decrease (i.e., more sustained constriction), compared with constant light, when increased activity of the modulated receptor results in increased encoded brightness, and vice versa.

Results

With an IR camera, pupil diameter was continuously measured for 30 min while participants viewed two temporally alternating silent substitution spectra (Fig. 1*A*). The spectra were designed so that one photoreceptor type (S-, M-, or L-cones or ipRGCs) was repeatedly exposed to illuminance increments and decrements

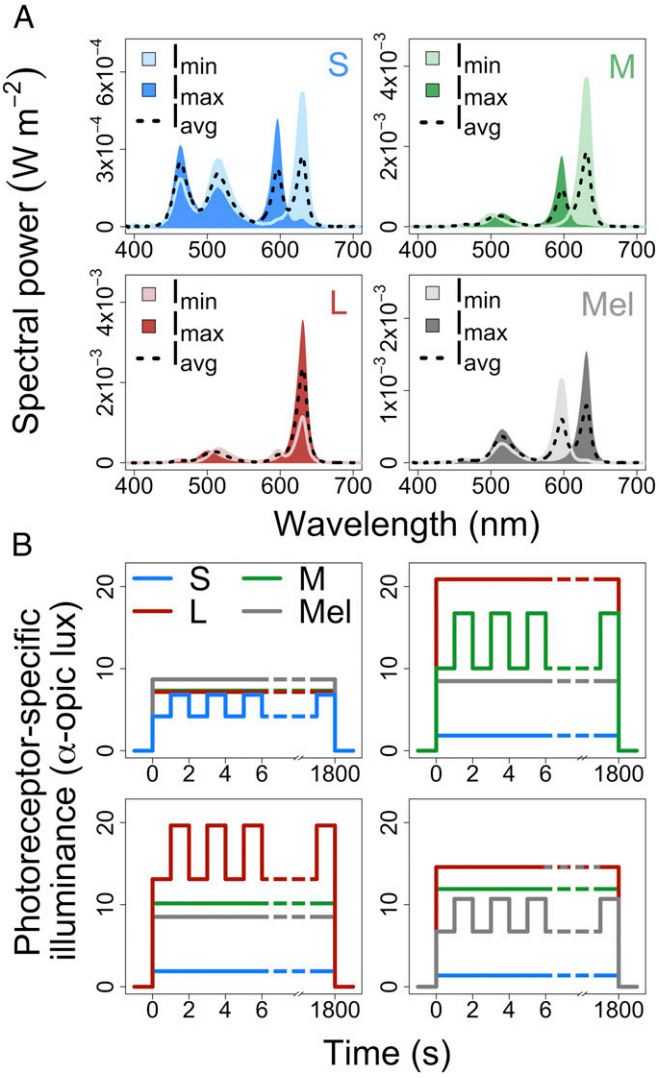

Fig. 1. Silent substitution spectra and protocol. (*A*) Silent substitution spectra per nonsilent photoreceptor. In each panel, the light and dark shaded areas correspond to I_{min} and I_{max}, respectively. Where the two spectra overlap, the solid line corresponds to the I_{min} spectrum. The dashed black line follows the average of I_{min} and I_{max}, which was used in the constant condition. (*B*) A schematic overview of photoreceptor-specific illuminance values for the 0.25-Hz condition. Separate panels show the spectra and protocols for the S- (*Top Left*), M- (*Top Right*), and L-cones (*Bottom Left*) and melanopsin (*Bottom Right*) modulations.

while illuminance values remained constant for all other receptors (Fig. 1*B*). The spectra were alternated at a frequency of 0.25, 0.5, 1, 2, or 4 Hz on separate occasions for each individual, with one modulated receptor per participant (four participants per modulated receptor).

To study the effect of photoreceptor-selective increments and decrements on pupil dilation, we calculated the event-related pupil response (ERPR). The ERPR represents the average pupil response to a photoreceptor-specific square-wave modulation. One ERPR was constructed per frequency condition per participant (Fig. 2). From these individual ERPRs, an average ERPR was created for each modulated photoreceptor, which are presented in Fig. 3 for the 0.25-Hz condition. For the L-cone and melanopsin modulating conditions, large-amplitude constrictions [0.64 ± 0.10 mm and 0.29 ± 0.04 mm, respectively (±SEM)] were measured in response to an illuminance increment ($P < 0.001$), whereas the pupil constriction in response to a decrement (0.07 ± 0.10 mm and

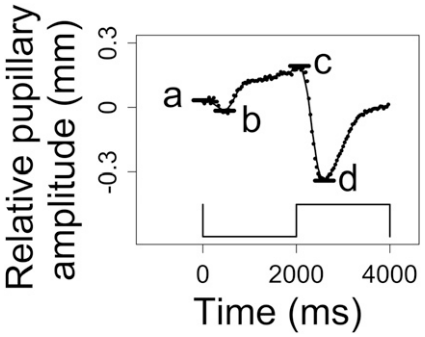

Fig. 2. Example ERPR for a representative participant who was exposed to the 0.25-Hz L-cone isolating flicker. The solid line follows the smoothed trend line that was used to calculate constriction amplitudes for statistical analyses. Horizontal line segments denote the local minima and maxima from which constriction amplitudes were calculated (*Methods and Materials*). Constriction to I_{min} and I_{max} were calculated as $|b - a|$ and $|d - c|$, respectively. Square-wave traces illustrate the photoreceptor-specific illuminance modulations.

0.03 ± 0.04 mm, respectively) did not reach significance. For the S-cone ($P < 0.01$) and M-cone ($P < 0.01$) modulating conditions, the largest constrictions were observed in response to decrements (0.25 ± 0.05 mm and 0.29 ± 0.05 mm, respectively), whereas the constriction induced by increments (0.07 ± 0.05 mm and 0.11 ± 0.05 mm, respectively) did not reach significance. ERPR amplitudes and test statistics are summarized in Table S1 for the 0.25-Hz condition. The ERPR results demonstrate that L-cone and melanopsin increments result in enhanced pupil constriction, whereas the opposite is observed for S-cone and M-cone increments. This phase reversal was observed for all frequency modulations (up to 2 Hz; Fig. 4), whereby maximal constriction was reached ∼500 ms after stimulus onset (L-cones and melanopsin) or offset (S- and M-cones).

By repeatedly incrementing and decrementing the illuminance for one photoreceptor over the course of 30 min, we expect that the net output of that photoreceptor remained at a high level as a result of adaptation processes. As a control, participants also viewed a nonmodulating stimulus that was the average of the incremental and decremental stimulus (Fig. 1*A*). Pupillary escape was thus expected to decrease compared with constant light (i.e., more sustained constriction) when an "excitatory" channel receives additional stimulation (Fig. 5*A*). The opposite was expected for an "inhibitory" channel, such that the pupil shows more dilation during the 30-min light exposure protocol. For each nonsilent photoreceptor, a linear regression model was constructed to explain pupil diameter by elapsed time (0–30 min) and modulation frequency. The interaction coefficients were then extracted as a quantification of pupillary escape for each modulation frequency (Fig. 5*B*). For the S-cone and M-cone conditions, all frequency modulations were associated with enhanced pupillary escape compared with the constant condition, although this effect was significant for only the 2-Hz condition for the S-cone ($P < 0.05$) and the M-cone ($P < 0.05$) modulations. For the L-cone and melanopsin conditions, all modulation frequencies resulted in a smaller pupillary escape compared with the constant condition, which was significant for all conditions ($P < 0.001$ and $P < 0.05$, respectively) except for the 0.05-Hz melanopsin condition. This implies that stimuli are encoded as being less bright when S- or M-cones receive additional activation. The opposite was found for L-cones or ipRGCs, such that the stimulus is encoded as being brighter by the pupillary control system when these receptors receive additional activation. Pupillary escape test statistics are summarized in Table S2.

Discussion

Recently, L- and M-cone opponent processing has been demonstrated to affect perceived brightness (7), the flicker ERG (8, 9), and VEPs at occipital scalp locations (10). In all these parameters, selective increments of L-cone illuminance are encoded as brightness increments, whereas M-cone increments are encoded as brightness decrements. S-cones have previously been reported to contribute negatively to visual luminance perception (14, 15). The ERPR results presented here extend this body of evidence to the domain of nonvisual photoreception by showing that the human pupillary control system encodes M-cone decrements and L-cone increments as brightness increments. We furthermore confirm the recently reported paradoxical pupillary constriction in response to S-cone decrements (5). L-cone and melanopsin responses were of an excitatory nature, such that increments in photoreceptor-specific illuminance were followed by pupil constrictions. Importantly, ipRGCs have been shown to be involved in visual brightness discrimination in mice and humans (16). This places our results in context with psychophysiological findings, with strong indications that nonvisual and visual brightness discrimination share a common pathway that starts in the retina. The large-amplitude ERPRs to L-cone modulations suggests a relatively large role for L-cones in the pupil response, which may be explained by the fact that the human retina expresses a relatively high number of L-cones in comparison with other receptors (17). Modulation of identical contrast for each receptor is therefore expected to result in relatively large-amplitude responses for L-cone–isolating modulations. The finding that, with higher-frequency modulations, the ERPR amplitude is dampened for all receptors likely reflects that, with increasing modulation frequencies, the pupil constriction dynamics become too sluggish to track the intensity modulations, resulting in dampened response amplitudes.

Interestingly, the dichotomy (S- and M-cones vs. L-cones and melanopsin) observed in the ERPR results was mirrored by the effects of photoreceptor-specific flicker on pupillary escape: S-cone and M-cone flicker increased pupillary escape (i.e., more dilation) whereas L-cone and melanopsin flicker resulted in a reduced pupillary escape (i.e., less dilation) compared with the constant light conditions. As the magnitude of pupillary escape is negatively correlated with light intensity (12), our findings raise the possibility that a flickering S-cone and M-cone modulating

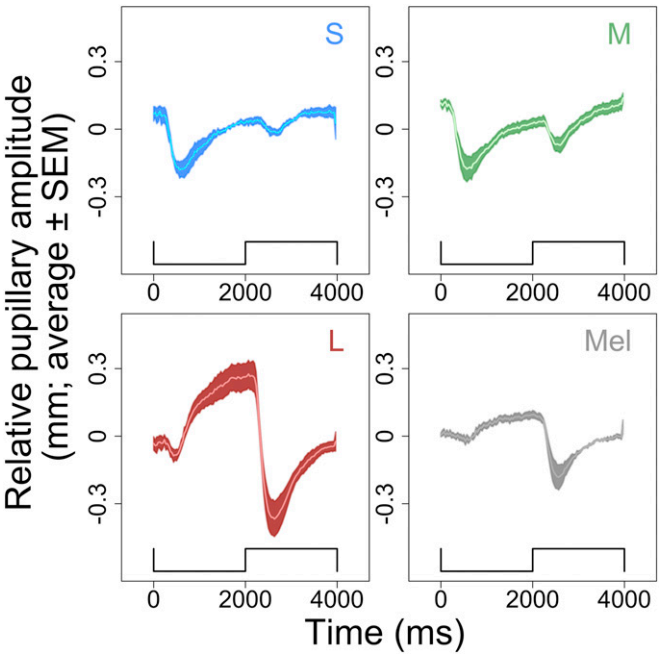

Fig. 3. Averaged ERPRs ± SEM. Each panel contains data from four participants. Separate panels show S-cone (blue), M-cone (green), L-cone (red), and melanopsin (gray) ERPRs. Square-wave traces illustrate the photoreceptor-specific illuminance modulations.

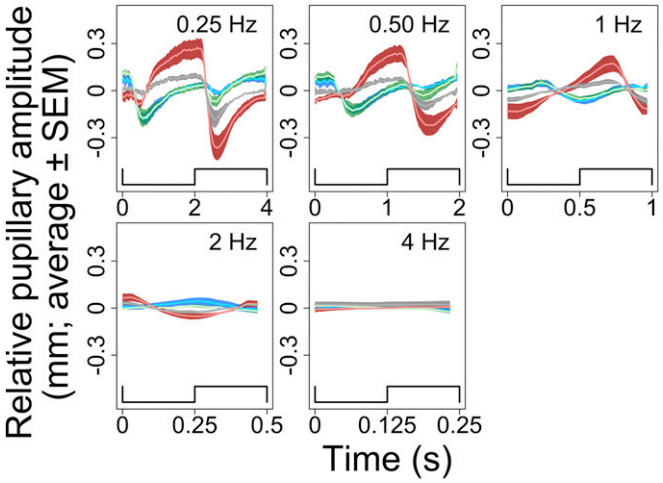

Fig. 4. ERPRs for the 0.25-Hz (*Top Left*), 0.5-Hz (*Top Middle*), 1-Hz (*Top Right*), 2-Hz (*Bottom Left*), and 4-Hz (*Bottom Right*) conditions. Square-wave traces illustrate the photoreceptor-specific illuminance modulations. Each panel contains data from all 16 participants (four participants per trace) except for the 1-Hz S-cone modulation, which contains data from three individuals (*Materials and Methods*).

light source is encoded as being less bright by the pupillary control system compared with constant light. The opposite appears to be true for the L-cone and melanopsin modulations under the employed intensities and frequency modulations. For cones, the frequencies resulting in the largest pupillary escape effects occur around frequencies of 1–2 Hz. Such frequency tuning was expected. Photoreceptors require enough time to dark-adapt to increase their sensitivity, while, at the same time, enough time in the light phase is required to evoke an increased overall response compared with light of constant intensity. The optimal trade-off between light and dark duration appears to lie in the 1–2 Hz range for pupillary escape, which has been reported previously (13). Our finding that effects on pupillary escape (Fig. 5) are significant only at a 2-Hz modulation for S- and M-cones is interesting, and suggests that long-term inhibitory S- and M-cone–mediated effects are more frequency-dependent than excitatory L-cone and melanopsin effects. Whether this is because of recruitment of different retinal circuits, or because pupillary escape effects for S- and M-cones are generally smaller (whereby relatively small effects transcend baseline noise only for the optimal frequency) remains to be validated by using electrophysiological experiments.

Although spectra were designed according to the method of silent substitution, photoreceptor-specific modulations should be interpreted as stimuli that are biased in favor of one photoreceptor type, as substitutions may not have been perfectly silent for the other types. This nuance is important because differences in photoreceptor spectral sensitivity are expected, as are differences in effective photoreceptor spectral sensitivity across the retina caused by the appearance of macular pigment in the fovea, mainly affecting short wavelength light (<500 nm). To explore how these factors may have affected our results, we performed 100 simulations, assuming peripheral (i.e., individual variation in peak spectral sensitivity of photoreceptors) or foveal retinal organization (i.e., assuming individual variation in photoreceptor sensitivity, individual variation in macular pigmentation, and different foveal photopigment optical densities). As melanopsin and rods are known to be practically absent in the fovea and are thus not affected by macular pigmentation, only S-, M-, and L-cone–specific illuminance values were simulated for the fovea. These simulations revealed that a difference in cone contrast may indeed be expected between the fovea and the peripheral retina. More importantly, however, in the fovea and in the periphery, stimuli were expected to be heavily biased toward the targeted photoreceptor (Tables S3 and S4), with minimal residual contrast for other receptor types (typically ∼1–2% contrast with ∼1–2% SD). It is therefore likely that all constrictions measured [including the unexpected insignificant but visually observable constriction in response to the minimum photoreceptor-specific illuminance (I_{min}) for the melanopsin condition] partially reflect the presence of residual cone contrast or apparent color changes, but that the large-amplitude constrictions mainly reflect the intended photoreceptor-modulations.

Our findings suggest that, in addition to the (L+M) − S color opponent ipRGCs (4), a subset of ipRGCs may receive color-opponent input on the red/green scale, with inhibitory and excitatory inputs from M-cone and L-cone–dominated pathways, respectively (i.e., +L − M). A similar statement can be made for a stimulus that shifts along the blue/cyan axis, where a blue-to-cyan shift results in a constriction and an opposite shift results in a dilation (+Mel − S). As there are +L − M but also −L+M midget ganglion cells, an explanation for our findings is that there are also +L − M and −L+M ipRGCs. Thus, although ipRGCs may be quite distinct from conventional RGCs [e.g., in the expression of melanopsin, dendritic field size (18), and S-off (L+M)/on responses (4)], red/green color discrimination may be a shared property of at least a subset of ipRGCs and midget ganglion cells. Our results are then likely explained by a higher number of +L − M ipRGCs. When these cells are the dominant response mediators when the stimulus shifts along the red/green scale, constrictions are expected for L-cone increments and M-cone decrements. An alternative is that the M-cone opposite-phase responses do not originate in the retina but may in fact be mediated by cortical processes. Although this possibility should not be neglected, the fact that opposite-phase M-cone responses are recorded at the level of the retina (8, 9) suggests that the results reported here reflect properties of retinal processing.

It is worth noting that, under a sine-wave modulation of M-cone illuminance, pupil diameter was previously not found to be out of phase with the M-cone illuminance modulation as we report here (19). This may result from methodological differences, as, in that

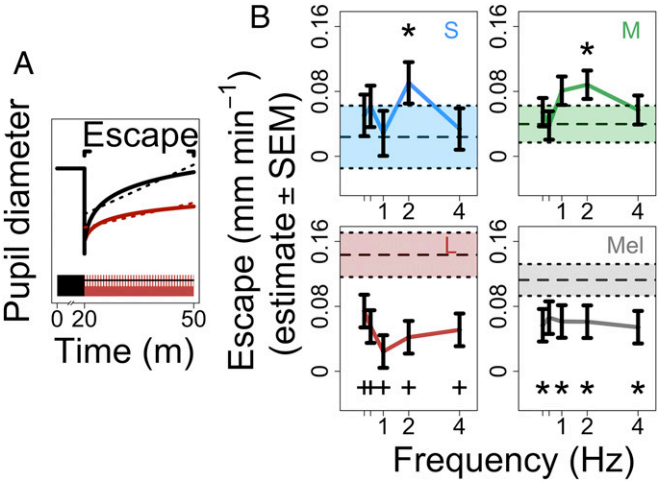

Fig. 5. Pupillary escape schematic illustration and results. (*A*) Schematic illustration of pupillary escape calculation under constant (black line; bottom) and L-cone–modulating (red trace; bottom) light. There is more pupillary escape in the constant condition, as the fitted slope for the constant condition is steeper than for the modulating condition. (*B*) Estimated (*Materials and Methods*) pupillary escape (mean ± SEM) over the 30-min light-exposure window. Each panel contains data from four participants. Separate panels correspond to the S- (*Top Left*), M- (*Top Right*), and L-cone (*Bottom Left*) and melanopsin (*Bottom Right*) modulations. The symbols indicate the significance level at which the estimated pupillary escape at each frequency modulation differs from the constant condition for each photoreceptor modulation separately (*$P < 0.05$ and $^{+}P < 0.001$). The colored shaded areas indicate the level of pupillary escape for the constant conditions (dashed line indicates estimated pupillary escape, dotted boundaries indicate ±SEM).

NEUROSCIENCE

study, the central 10.5° of a circular 30° visual field was blocked. Based on our simulations (Tables S3 and S4), it is not expected that the opposite-phase M-cone responses are an artifact of incomplete silencing of foveal cones. A more parsimonious explanation is that variations along the red/green scale are most efficiently encoded at the fovea, with a decline toward the periphery (20). This decline in red/green sensitivity (+L − M or −L+M mediated) is steeper than for luminance (mediated by L+M channels). It is therefore possible that M-cone–modulating stimuli applied to the periphery predominantly feed into the achromatic luminance pathway (L+M) instead of the red/green chromatic pathway. Hence, an M-cone increment delivered at the periphery will induce a larger response in the (L+M) − S ipRGCs than in the putative +L − M ipRGCs, resulting in pupil constriction.

It is important to consider that the rods were not silenced in any of the silent substitution pairs, which may have influenced our results, as, in mice, it has been shown that rods persist signaling at higher intensity levels than was previously thought (21). However, recent reports showed that, in humans, rod-inducible pupil constrictions were measurable only at low light levels that are consistent with the human rod-saturation threshold determined previously (22). The lowest scotopic intensity used in the present study was 7.75 lx (I_{max} spectrum for the L-cone condition), which translates to 2.15 log scotopic trolands (sc td) at a pupil diameter of 3.13 mm (i.e., the average pupil diameter recorded over all testing sessions). At this background illumination level, increments in illuminance are not perceived via the scotopic system, which has been shown to saturate at ∼1.0–1.5 log sc td under similar conditions (23). Thus, as rods are expected to be saturated at the light intensities employed here, it is also expected that rods are incapable of responding to illuminance modulations under these conditions in humans. Similarly, it is unlikely that rod-specific illuminance modulations have resulted in repeated relative dark- and light-adaptation, and that the pupillary escape effects are the result of adaptation processes in rods. Therefore, with the light intensities used in the present study, it is unlikely that rod intrusions have contaminated the results presented here.

Our results provide important insights into the functional retinal organization that affects brightness coding in nonvisual light responses. Such advances may prove to be important in understanding brightness coding in other nonvisual responses mediated by ipRGCs, such as modulation of alertness, melatonin suppression, and timing of the sleep/wake cycle.

Materials and Methods

Participants. For this study, 16 healthy young participants (10 female, six male), aged 22.13 ± 2.09 y (average ± SD; range, 19–25 y) were recruited. Participants were screened for color blindness by performing an Ishihara color blindness test. Failure to complete this test without errors was a direct exclusion criterion.

Pupillometer. Pupil diameter was measured simultaneously from both eyes at a sampling frequency of 30 Hz by using an Eyetribe eye tracker (The Eye Tribe ApS) consisting of high-frequency IR LED illumination and a camera allowing for quantification of pupil diameter (in camera pixels). To convert camera pixels into pupil diameter in millimeters, a calibration procedure was performed in which pupil diameter was simultaneously measured with the eye tracker (in pixels) and a separate pupillometer that expresses pupil diameter in millimeters (PLR-2000 Pupillometer; NeurOptics). At a distance of 40 cm between the eye tracker and the center between both eyes (i.e., the distance that was also maintained in the experiment by a chin rest), one pixel corresponded to 0.13 mm.

Light Box. The light source used was an in-house developed light box. LEDs of five different colors (blue, cyan, green, yellow, and red; Fig. S1) were controlled separately via an Arduino Uno microcontroller. For each light channel, the intensity was controlled digitally (range, 0–255) via pulse-width modulation. The LED panel was placed in a nontransparent plastic box with a flat spectrum diffuser, required to obtain a uniform distribution of color and intensity over the light-emitting surface of the light box.

Silent Substitution. The method of silent substitution (6) is based on the principle of univariance, which states that two different light spectra will affect a given photoreceptor cell identically, as long as the number of photons absorbed by its opsins is also identical between the two. This principle makes it possible to extract photoreceptor-specific illuminance values from any light spectrum by correcting the spectrum for prereceptoral filtering, the known absorption curves for each opsin, and finally the peak axial optical density of individual photoreceptors. A recently developed method that accounts for all of these factors was used to calculate photoreceptor-specific illuminance, expressed in lux (24). In the present study, whenever illuminance values were calculated, this method was used. When a light spectrum with a given set of photoreceptor-specific illuminance values is substituted for a different spectrum with the same set of illuminance values, none of the photoreceptors will be affected differently (i.e., substituting one spectrum for the other is silent for all photoreceptors). Similarly, it is possible to design a pair of spectra that can be silently substituted for all but one photoreceptor, granting independent control over the photoreceptor for which the substitution is nonsilent. The previously described light box was designed to produce such pairs of silent substitution spectra. The typical strong linear relationship between LED intensity and each photoreceptor-specific illuminance value allows for prediction of the photoreceptor-specific illuminance values that the light box will produce, given a certain configuration of intensity settings. Importantly, the reverse is also true: given a desired set of photoreceptor-specific illuminance values, it is possible to calculate the required intensity level for each LED color that would produce a spectrum with these illuminance values. With the use of a mixed-integer linear programming solver ("lpSolveAPI" package in R, version 3.2.3), the light intensity configuration settings required to obtain four pairs of silent substitution spectra were calculated, whereby each pair was nonsilent for one of the S-, M-, L-cone or melanopsin photopigments. The solver was run with the constraint that the Michelson contrast for the nonsilent photoreceptor was always 23% [Michelson contrast was calculated as $(I_{max} - I_{min})/(I_{max} + I_{min})$ where I denotes the photoreceptor-specific illuminance]. Michelson contrast describes the contrast of a periodic signal relative to its average value, and is a universally accepted metric of luminance contrast (25). In addition, the amount of melanopic lux for the three pairs of cone-specific silent substitution spectra was always set to ∼8.5 to control for the substantial melanopsin-mediated contribution to the sustained pupillary light response (12). The average amount of melanopic lux over the two melanopsin-specific silent substitution spectra was also set to this level while maintaining the 23% contrast between minimal and maximal melanopic illuminance. Finally, the rods were not silenced, as these were expected to be saturated at intensities employed here (*Discussion*). All spectra were validated with a spectroradiometer (SpecBos 1211 LAN UV; JETI Technische Instrumente). The spectra for each of the silent substitution pairs are presented in Fig. 1*A*. An overview of the measured photometric properties of the silent substitution spectra is provided in Table S3.

Experimental Protocol. The study took place in the human research facility of the Groningen Institute for Evolutionary Life Sciences at the University of Groningen, The Netherlands. The time of measurement was at daytime, limited to five time slots: 0900–1000 h, 1030–1130 h, 1200–1300 h, 1330–1430 h, and 1500–1600 h, where only one time slot was allowed per participant to minimize time of day effects. Participants (10 female, six male) were seated in isolated rooms in which light, sound, and temperature conditions were regulated. Participants were asked to perform six testing sessions (one session per condition; *Study Design*) with a minimum of 2 d in between two testing sessions. At the start of each session, participants were seated in front of a desk, facing the light-emitting surface of the light box and the eye tracker. Movement artifacts were minimized with the use of a chin rest. The height of the chin rest was adjusted to achieve horizontal alignment between the center of the eyes and the center of the light box. The distance between the eyes and the light box was 40 cm for all individuals. At this distance, the angular size of the light-emitting surface (17.5 × 8.5 cm) was 24.68° horizontally and 12.13° vertically. Participants were asked to remain seated as still as possible for the rest of the testing session while fixating on the center of the light box, which was marked with a 5 × 5-mm cross-hair. When the participant was ready, the eye tracker was set to record the pupil diameter, and the experimental protocol started with a 20-min dark adaptation period. After 20 min, the 30-min light schedule (corresponding to the condition the participant was assigned to for each particular testing session) started. After the light schedule was finished, the pupil recording was stopped, and the data, consisting of one file containing timing of intensity configurations sent to the light box and one file containing pupil diameter measurements at a frequency of 30 Hz, were collected.

Study Design. The study followed a between/within subject design with nonsilent photoreceptor as between-subject and frequency modulation as within-subject factors. The 16 participants were divided in groups of four in which a different photoreceptor was targeted for each group. In five of the six testing sessions,

individuals were exposed to a pair of silent substitution spectra that alternated in a square-wave fashion at a frequency of 0.25, 0.5, 1, 2, or 4 Hz. In the remaining session, individuals were exposed to light of constant intensity and spectral composition. In the constant light condition, the illuminance for the silenced photoreceptors was identical to the illuminance levels in both silent substitution spectra, whereas the illuminance for the nonsilent photoreceptor was now fixed at the average illuminance level of I_{max} and I_{min}. Within each group of four participants, the order of conditions was constant, 0.25, 0.5, 1, 2, and 4 Hz for two individuals, and, for the other two individuals, the order was reversed. Fig. 1*B* provides an example for the 0.25-Hz condition for all photoreceptor conditions.

Artifact Removal. All data preprocessing was performed in R (version 3.2.3; Rstudio version 1.0.136). For the pupil diameter data, samples containing unreliable data were excluded from the dataset (for each individual testing session separately). These unreliable samples were primarily recognized by an absolute difference of >5 pixels between the pupil diameters of both eyes. This threshold was chosen because 95% of the data contained samples in which the absolute difference in pupil size was <5 pixels, and, in case of a steady signal, the pupil diameters of both eyes were visually consistently observed to be <5 pixels apart for all individuals. Samples in which at least one of the two pupil diameter values was missing were also considered unreliable samples and were removed accordingly. These instances occurred when the pupil was partially covered by the eyelid, during eye blinks, and during movement. Next, additional artifacts that were not recognized by the procedures already described were identified and removed via a local polynomial regression fitting procedure ["loess" function in R (26)]. With this procedure, a smoothed trend line was fitted through the data points, after which the residuals were extracted. Residuals >1.5 interquartile range above or below the upper and lower quartiles of the residual distribution, respectively, were identified as outliers and removed from the dataset. For each sample, pupil diameter was calculated as the average pupil diameter of both eyes. Next, the pupil data were synchronized with the light-stimulus event log files. For one individual (S-cone modulation, 1-Hz condition), no usable data remained after artifact removal. This subset of the data were therefore removed from further analysis procedures.

ERPRs. To construct ERPRs, the timing of each sample was first expressed relative to the latest onset of I_{min} for each sample. The average pupil diameter was then calculated for each of these relative time points, revealing the typical (i.e., average) pupil diameter trace for an $I_{min} - I_{max}$ cycle. Relative pupillary amplitude was then calculated by subtracting the average of each individual trace from each constituent (i.e., averaged) data point, which yielded an ERPR with a mean of 0 for each individual separately. The amplitude of constriction in response to I_{min} and I_{max} was calculated for each individual separately. To do this, a loess trend line was fitted through the individual ERPRs (Fig. 2). From the smoothed trend line, maxima and minima were determined for I_{min} and I_{max}. Constriction amplitudes were then calculated as the absolute difference between the maximum and the minimum pupil size for I_{min} and I_{max} separately.

Pupillary Escape. For the analysis of pupillary escape, the data from each individual testing session were smoothed by averaging pupil diameter over bins of 30 s. Only the data obtained during the light intervention period were included.

Statistical Procedures. All statistics were analyzed in R (version 3.2.3; Rstudio version 1.0.136). A critical significance level (α) of 0.05 was maintained for all analyses. For the ERPR results, only the slowest frequency employed (0.25 Hz) was statistically analyzed because, in the other conditions, we observed intrusion of pupil responses (which are relatively slow) to I_{max} into the I_{min} window and vice versa. For the other conditions, the ERPR traces are provided in Fig. 4 as a reference. For the analysis of constriction amplitudes, four (one for each nonsilent photoreceptor) simple regression models (base function "lm" in R) were constructed. In these models, the independent variable was illuminance level (I_{min} vs. I_{max}) and the dependent variable was pupil constriction amplitude. For these regression models, two-tailed *P* values were calculated. Pupillary escape was estimated for each combination of photoreceptor/frequency modulation separately via a mixed linear regression approach by using the "lme4" package in R (27). Models were created for each nonsilent photoreceptor separately with time, frequency modulation, and the interaction term as fixed effects. To account for individual random variation in pupil diameter and pupillary escape, a random intercept and random slope was included in the model at the level of participant ID. For each model, the interaction contrasts were subjected to a multiple comparison procedure ("multcomp" package in R). This procedure effectively tests whether the change in pupil diameter over time for each of the flickering conditions is significantly different from the change over time in the constant light condition.

Data Availability. Original data, analyses, and R codes can be accessed by contacting the corresponding author. The complete dataset (original and analyzed) and R codes are also available at the data repository at the University of Groningen.

Ethics Statement. The study procedures were approved by the medical ethical research committee of University Medical Centre Groningen (protocol NL53779.042.15) and are in accordance with the Declaration of Helsinki (2013). All participants gave written informed consent.

ACKNOWLEDGMENTS. We thank all subjects for participating in the experiment and Gerard Overkamp for his help in developing the LED box. This work was funded by Nederlandse Organisatie voor Wetenschappelijk onderzoek/Stichting voor de Technische Wetenschappen OnTime Program Grant 10.13039/501100003958 (project 12187).

1. Lee BB (2011) Visual pathways and psychophysical channels in the primate. *J Physiol* 589:41–47.
2. Güler AD, et al. (2008) Melanopsin cells are the principal conduits for rod-cone input to non-image-forming vision. *Nature* 453:102–105.
3. Berson DM, Dunn FA, Takao M (2002) Phototransduction by retinal ganglion cells that set the circadian clock. *Science* 295:1070–1073.
4. Dacey DM, et al. (2005) Melanopsin-expressing ganglion cells in primate retina signal colour and irradiance and project to the LGN. *Nature* 433:749–754.
5. Spitschan M, Jain S, Brainard DH, Aguirre GK (2014) Opponent melanopsin and S-cone signals in the human pupillary light response. *Proc Natl Acad Sci USA* 111:15568–15572.
6. Estévez O, Spekreijse H (1982) The "silent substitution" method in visual research. *Vision Res* 22:681–691.
7. Parry NRA, McKeefry DJ, Kremers J, Murray IJ (2016) A dim view of M-cone onsets. *J Opt Soc Am A Opt Image Sci Vis* 33:A207–A213.
8. McKeefry D, et al. (2014) Incremental and decremental L- and M-cone-driven ERG responses: I. Square-wave pulse stimulation. *J Opt Soc Am A Opt Image Sci Vis* 31:A159–A169.
9. Kremers J, et al. (2014) Incremental and decremental L- and M-cone driven ERG responses: II. Sawtooth stimulation. *J Opt Soc Am A Opt Image Sci Vis* 31:A170–A178.
10. Barboni MTS, et al. (2017) L-/M-cone opponency in visual evoked potentials of human cortex. *J Vis* 17:20.
11. Bartley SH (1939) Some effects of intermittent photic stimulation. *J Exp Psychol* 25: 462–480.
12. Gooley JJ, et al. (2012) Melanopsin and rod-cone photoreceptors play different roles in mediating pupillary light responses during exposure to continuous light in humans. *J Neurosci* 32:14242–14253.
13. Vartanian GV, Zhao X, Wong KY (2015) Using flickering light to enhance nonimage-forming visual stimulation in humans. *Invest Ophthalmol Vis Sci* 56:4680–4688.
14. Lee J, Stromeyer CF, 3rd (1989) Contribution of human short-wave cones to luminance and motion detection. *J Physiol* 413:563–593.
15. Stockman A, MacLeod DI, DePriest DD (1991) The temporal properties of the human short-wave photoreceptors and their associated pathways. *Vision Res* 31:189–208.
16. Brown TM, et al. (2012) Melanopsin-based brightness discrimination in mice and humans. *Curr Biol* 22:1134–1141.
17. Hofer H, Carroll J, Neitz J, Neitz M, Williams DR (2005) Organization of the human trichromatic conemosaic. *J Neurosci* 25:9669–9679.
18. Do MTH, Yau K-W (2010) Intrinsically photosensitive retinal ganglion cells. *Physiol Rev* 90:1547–1581.
19. Cao D, Nicandro N, Barrionuevo PA (2015) A five-primary photostimulator suitable for studying intrinsically photosensitive retinal ganglion cell functions in humans. *J Vis* 15:15.1.27.
20. Hansen T, Pracejus L, Gegenfurtner KR (2009) Color perception in the intermediate periphery of the visual field. *J Vis* 9:26.1-12.
21. Altimus CM, et al. (2010) Rod photoreceptors drive circadian photoentrainment across a wide range of light intensities. *Nat Neurosci* 13:1107–1112.
22. Barrionuevo PA, Cao D (2016) Luminance and chromatic signals interact differently with melanopsin activation to control the pupil light response. *J Vis* 16:29.
23. Adelson EH (1982) Saturation and adaptation in the rod system. *Vision Res* 22:1299–1312.
24. Lucas RJ, et al. (2014) Measuring and using light in the melanopsin age. *Trends Neurosci* 37:1–9.
25. Switkes E, Crognale MA (1999) Comparison of color and luminance contrast: Apples versus oranges? *Vision Res* 39:1823–1831.
26. Cleveland WS, Grosse E, Shyu WM (1992) Local regression models. *Statistical Models in S*, eds Chambers JM, Hastie TJ (Chapman and Hall, London), pp 309–376.
27. Bates D, Mächler M, Bolker B, Walker S (2015) Fitting linear mixed-effects models using lme4. *J Stat Softw* 67:1–48.